RSC Advances

PAPER

View Article Online
View Journal | View Issue

Check for updates

Cite this: *RSC Adv.*, 2019, **9**, 21572

Novel designed azo substituted semi-cyanine fluorescent probe for cytochrome P450 reductase detection and hypoxia imaging in cancer cells†

Caiyue Wang,[ab] Shuping Zhang,*[a] Junhai Huang,[b] Lei Cui,[c] Jin Hu[b] and Shaoying Tan *[b]

Received 11th April 2019
Accepted 30th June 2019

DOI: 10.1039/c9ra02741f

rsc.li/rsc-advances

A hypoxia activated fluorescent probe **AZO-Cy** which contains an azo group conjugated to the electron withdrawing part of the fluorescent dye was synthesized. In the presence of NADH, **AZO-Cy** displayed high selectivity and sensitivity to cytochrome P450 reductase (CPR) under low p_{O_2}. The probe showed high anti-interference capability in the presence of other biothiols and ions. In A549 cell imaging, the fluorescence intensity is increased about 11-fold under hypoxia compared to normoxia conditions. Further inhibitor experiments showed that CPR is not the only reductase that can take part in the process of azo bond reduction. The probe **AZO-Cy** displayed high oxygen sensitivity in the identified different hypoxic status of tumor cells which provides huge potential application toward *in vivo* hypoxia detection.

Open Access Article. Published on 11 ervence 2019. Downloaded on 17.12.2025 17:34:02.
This article is licensed under a Creative Commons Attribution-NonCommercial 3.0 Unported Licence.

1. Introduction

Low oxygen concentration or insufficient oxygen supply which means hypoxia is a major phenomenon in various diseases. Oxygen plays an important role in the balance of pathological and physiological processes.[1–6] Normally, the hypoxic area means a p_{O_2} value ≤2.5 mm Hg which can be found in solid tumors, cardiac ischemia and inflammatory diseases. Clinical research has found that the hypoxic environment in solid tumors has a certain relationship to the tumor cells' resistance to treatment and metastasis.[7,8] Because of the inadequate supply of oxygen, there is not enough oxygen transferred to reactive oxygen species (ROS) in a hypoxic environment. In this condition, the reduction of ROS concentration means the increase in reducing ability. Groups such as aromatic nitro group, azo group and quinone group have been applied in the designing of various hypoxic activated fluorescent probes.[9–12] So far, various methods have been applied in the detection of hypoxia in the clinic, including positron emission tomography/computed tomography (PET/CT), electron paramagnetic resonance imaging (EPRI) and so on.[13–15] Because it is non-invasive, and has high sensitivity and high spatiotemporal resolution, fluorescence imaging is still an ideal method for hypoxia detection.[16–20]

As a metabolism enzyme, cytochrome P450 reductase plays a key role in the reduction of nitro functional compounds and has higher activity in cancerous cells than in normal cells, especially in a hypoxic environment. Several studies have proved that azo aromatic compounds are good substrates for cytochrome P450 reductase.[18,20–23] Some fluorescent probes showed good performance under different oxygen partial pressures which meant the azo group was very effective to detect hypoxia. Based on our previous work,[19] herein, we report a far-red emitting probe **AZO-Cy** containing an azo moiety which can be metabolized by cytochrome P450 reductase in hypoxic conditions, the probe displayed a strong fluorescence OFF–ON response at 610 nm in PBS buffer and in hypoxia imaging in tumor cells.

2. Experimental section

2.1 Instruments and chemicals

UV-visible absorption spectra were obtained using a UV-visible spectrometer (Scinco 3000 spectrophotometer). Fluorescent spectra were performed on a Hitachi F-7000 luminescence spectrophotometer in 10 × 10 mm quartz cells with the volume 3.0 mL at 37 °C. ^{1}H and ^{13}C spectra were measured using a Bruker ARX 400 NMR spectrometer. The molecular mass was acquired using ion trap time-of-flight mass spectrometry (MS-TOF). Fluorescence imaging experiments were performed on a confocal microscope (Olympus, IX81, JPN). A liquid chromatography system from Waters Technologies (Waters, American) was applied to all chromatography tests.

[a]*College of Science, University of Shanghai for Science and Technology, Shanghai, China*

[b]*State Key Laboratory of New Drug and Pharmaceutical Process, Shanghai Institute of Pharmaceutical Industry, China State Institute of Pharmaceutical Industry, 1599 Zhangheng Road, Shanghai, 201203, China. E-mail: tanshaoying2019@163.com*

[c]*College of Science, Shanghai University, Shanghai, China*

† Electronic supplementary information (ESI) available. See DOI: 10.1039/c9ra02741f

This journal is © The Royal Society of Chemistry 2019

Open Access Article. Published on 11 ervence 2019. Downloaded on 17.12.2025 17:34:02.
This article is licensed under a Creative Commons Attribution-NonCommercial 3.0 Unported Licence.

All of the chemicals and solvents were purchased from commercial suppliers and used without further purification, unless otherwise stated. Deionized water was used to prepare all aqueous solutions.

2.2 Preparation of probe AZO-Cy

Probe **AZO-Cy** was synthesized from the commercially available starting material **1-1** as shown in Scheme 2. The key intermediates and probe **AZO-Cy** were confirmed using ^{1}H NMR, ^{13}C NMR and HR-MS (see ESI†).

Synthesis of AZO-Cy. Compound **1** (300.0 mg, 1.0 mmol) and nitrosobenzene (627.0 mg, 5.9 mol) were dissolved in acetic acid (4 mL). Then the mixture was stirred at 25 °C for 5 h. 10 mL water was added and then the mixture was extracted with methylene chloride (10 mL × 3). The combined organic layers were washed with brine and dried over anhydrous Na_2SO_4. Then the solvent was concentrated in vacuum and the residue was purified using silica gel chromatography (DCM : MeOH = 20 : 1, v/v) to provide **AZO-Cy** (100 mg, 26%) as a bright purple-black solid. ^{1}H NMR (400 MHz, DMSO-d_6) δ 8.10 (d, J = 1.7 Hz, 1H), 8.06–7.96 (m, 2H), 7.96–7.82 (m, 4H), 7.64–7.58 (m, 2H), 7.58–7.51 (m, 2H), 6.76 (d, J = 14.4 Hz, 1H), 6.41 (d, J = 8.8 Hz, 2H), 5.76 (s, 1H), 4.29 (q, J = 6.8 Hz, 2H), 1.99 (s, 1H), 1.76 (s, 6H), 1.32 (t, J = 7.0 Hz, 3H), 1.27–1.13 (m, 3H). ^{13}C NMR (101 MHz, DMSO-d_6) δ 184.13, 168.27, 152.16, 148.29, 146.05, 145.11, 141.62, 130.85, 129.42, 126.53, 124.89, 122.46, 122.28, 114.75, 109.64, 96.79, 47.44, 37.88, 27.51, 11.98. HRMS (ESI$^+$) calcd for $C_{26}H_{26}N_3O^+$ $[M]^+$ = 396.2070, found 396.2066.

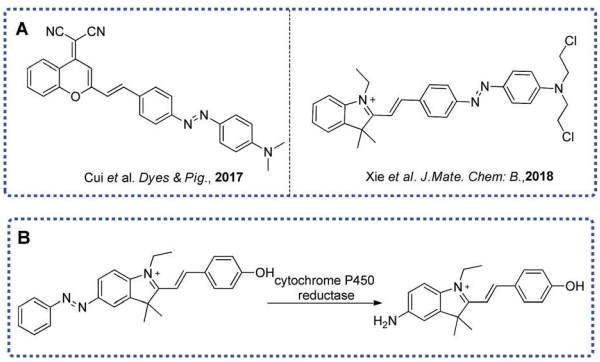

Scheme 1 Previously reported probes (A) and current work (B).

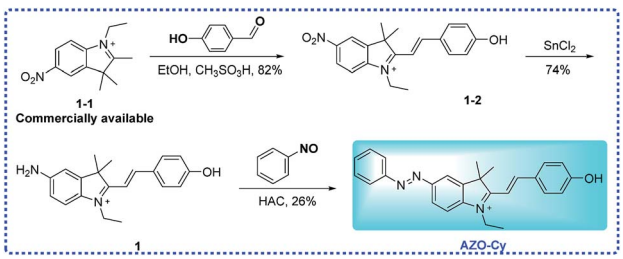

Scheme 2 Synthesis of **1** and probe AZO-Cy.

2.3 Spectroscopic materials and methods

Double distilled water was used to prepare all aqueous solutions. All spectroscopic measurements were performed in PBS buffer (1% DMSO, 0.1 mM, pH = 7.4). Samples for absorption and fluorescence measurements were contained in 1 cm × 1 cm quartz cuvettes (1.5 mL volume) by setting the slit width of 3 nm × 1.5 nm.

2.4 Cytochrome P450 reductase assay

Cytochrome P450 reductase (rabbit liver, purchased from Sigma-Aldrich, CPR) reactive activity experiments were performed in a 1 cm × 1 cm quartz cuvette with 100 μL volume. Stock solutions of probe **AZO-Cy** were prepared in pure DMSO (1 mM). All experiments were performed in PBS buffer (0.1 mM, pH = 7.4) in 37 °C water bath. The dosage of cytochrome P450 reductase is 1 U mL^{-1}. Argon gas mixtures with different p_{O_2} were bubbled into the **AZO-Cy** solution for 30 min to create the different hypoxic environments.

2.5 Cell culture and confocal microscope imaging

A549, purchased from American Type Culture Collection (ATCC, Manassas, VA, USA), was chosen for culturing with RPMI-1640 (Hyclone), supplemented with 10% FBS (fetal bovine serum, Gibco), 2 mM L-glutamine, 100 U mL^{-1} penicillin and 100 μg mL^{-1} streptomycin in an atmosphere of 5% CO_2 and 95% air (37 °C). Cells were seeded in the 24-well plates at a density of 1 × 10^5 in a culture medium. For fluorescence imaging, cells were divided into two parts, one part was incubated under different hypoxic (1% p_{O_2}) conditions and the other part was under normoxic conditions (21% p_{O_2}) for 24 hours, respectively. Then, after washing with PBS buffer twice, the cells were treated with **AZO-Cy** in FBS-free RPMI-1640 for 30 min before fluorescence imaging, respectively. The pictures were collected with a Nikon instrument (Eclipse Ti-E2000). The fluorescence field was collected with 200 ms exposure time using a Texas Red filter and with 100 ms exposure time for bright field.

3. Results and discussion

3.1 Synthesis and structural characterization

Previously, our group have developed a series of hypoxic activated fluorescent probes which were based on different functional group, including benzoquinone, aromatic nitro group and azo group.[24,25] We found that the azo bond is more sensitive than other functional group under hypoxic conditions, such as a nitro group, benzoquinone and N–O bond. Most of the probes' functional groups were linked to the electron-rich side (phenolic hydroxyl group or aromatic amino) directly or by a linker. Here, the designed probe **AZO-Cy** contains an azo group which is connected to the indole group (electron-withdrawing part) directly. Probe **AZO-Cy** displayed a dramatic optical change as well as high sensitivity to cytochrome P450 reductase.

3.2 UV-vis and fluorescence study

The UV-vis spectra and fluorescence spectra of **AZO-Cy** were monitored in PBS buffer. From Fig. S1,† we can find that the

Open Access Article. Published on 11 ervence 2019. Downloaded on 17.12.2025 17:34:02.
This article is licensed under a Creative Commons Attribution-NonCommercial 3.0 Unported Licence.

absorption spectra of both compounds only showed minor differences. In contrast, the fluorescence spectra showed great differences. No fluorescence signal could be detected for the probe **AZO-Cy**, but an obvious signal at the wavelength of 610 nm was detected for the reduced dye **1**. This means compound **AZO-Cy** showed great application potential in the detection of cytochrome P450 reductase with fluorescence (Table S1†).

3.3 Spectrum of probe AZO-Cy towards cytochrome P450 reductase

Cytochrome P450 reductase plays key roles in the detoxification and activation of xenobiotics and has been widely applied in the metabolism of organic molecules such as drugs, pesticides, plant toxins, and mutagens. Until now, several research studies, including from our group, have proven that the enzyme shows a strong reducing ability that could reduce azo compounds under hypoxic conditions. Here, the new designed probe has a significant difference in chemical structure, as shown in Scheme 1, to most of the reported probes, where the functional group was connected to the electron-donating end of the fluorophore molecule.[9,16,19,23] Here, the azo group of the probe **AZO-Cy** connected to the electron-withdrawing end which is a first report.

As shown in Fig. 1, nearly no fluorescence signal at 610 nm was detected because of the vibration of the azo bond in probe **AZO-Cy**. After enzyme CPR was added, we monitored the fluorescence changes of **AZO-Cy** (10 μM in PBS, pH 7.4, $\lambda_{ex} = 450$ nm) after the additions of CPR (1.0 U mL^{-1}) and NADH (100 μM) (Fig. 1b). A significant signal emission was detected at 610 nm and enhanced about 15-fold. The detected fluorescence intensity of **AZO-Cy** displayed a concentration-dependent and time-dependent increase. After probe **AZO-Cy**, CPR and NADH reacted for 5 min, the fluorescence intensity only showed a slight increase which suggested a rapid response to enzyme CPR (Fig. 1a).

For an inhibitor assay, diphenyliodonium chloride (DPIC) was chosen as a reported inhibitor of CPR,[27] and was added to the enzyme prior to the incubation of **AZO-Cy**, and the inhibitory effect on CPR was investigated. The incubation of DPIC (100 μM) in a mixture of **AZO-Cy**, CPR and NADH led to a very weak fluorescence signal (Fig. 1b and c), the signal intensity of which was twelve times lower than **AZO-Cy** expressed in the presence of CPR and NADH, due to the competitive inhibition of DPIC to the enzymatic action (Fig. 1c). The experiment also proved that the coenzyme NADH is also a key factor in the enzyme-catalyzed reduction.

For accurate measurement of the real activities of CPR in various biological samples and to get the linear fluorescence response with enzyme concentration, kinetic experiments were also investigated. The kinetics of the release of **1** from **AZO-Cy** triggered by CPR in the presence of NADH was measured by adding a known concentration of **AZO-Cy** (0–100 μM) to the reaction mixture. The fluorescence change was recorded at the

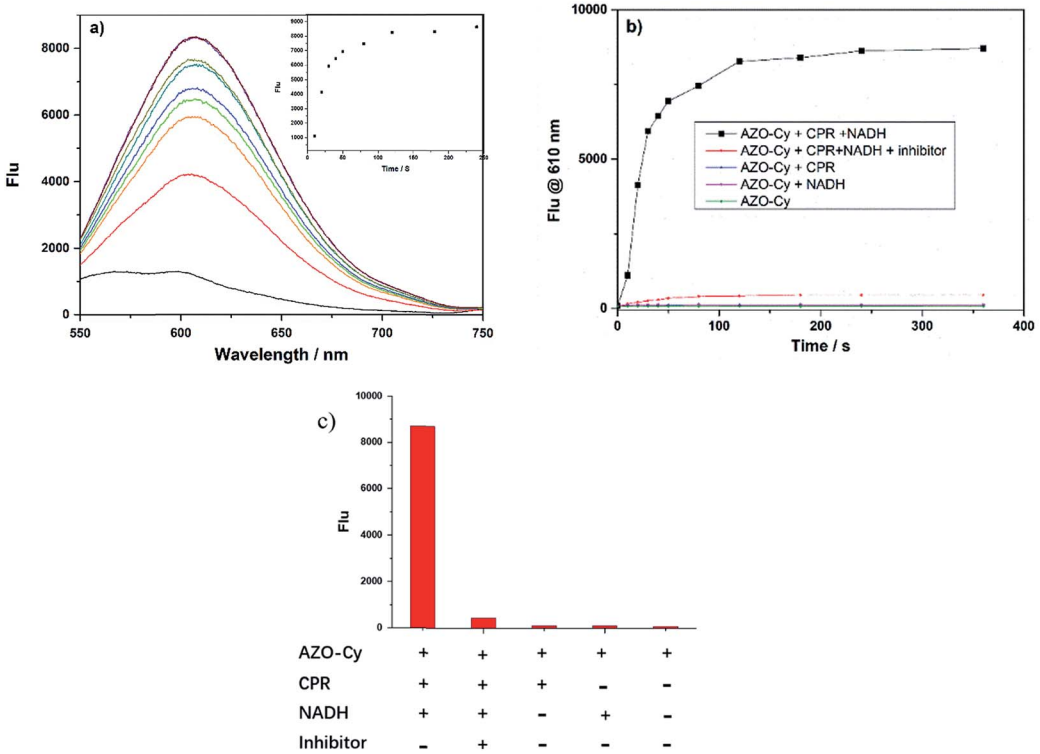

Fig. 1 Activity of probe **AZO-Cy** towards cytochrome P450 reductase. (a) Fluorescence spectra of probe **AZO-Cy** (10 μM) incubated in the presence of CPR (1.0 U mL^{-1}) and NADH (50 μM) in PBS buffer at 37 °C; (b) time dependent fluorescence changes of probe in various conditions and (c) their fluorescence responses ($\lambda_{ex} = 450$ nm, 6 min). Probe **AZO-Cy** (10 μM) was incubated in the presence of CPR (1.0 U mL^{-1}), NADH (50 μM), or an inhibitor (DPIC, 100 μM) at 37 °C.

 This journal is © The Royal Society of Chemistry 2019

Open Access Article. Published on 11 ervence 2019. Downloaded on 17.12.2025 17:34:02.
This article is licensed under a Creative Commons Attribution-NonCommercial 3.0 Unported Licence.

wavelength of 610 nm, all assays were performed in triplicate, and the results reported are the average of three experiments (Fig. 2).

Probe **AZO-Cy** shows high reaction activity to CPR with NADPH which is faster than reported before.[18,20,26–28] Experiments show that after mixing for 2 min, the fluorescence signal can reach a maximum, which provides the basis for rapid response detection of hypoxia (Table S2†). The mechanism of the reduction of probe **AZO-Cy** by CPR was also confirmed by HPLC (Fig. S3†). With the passage of reaction time, the concentration of **AZO-Cy** (retention time was 5.68 min) decreased obviously, and it almost disappeared after about 5 min (Fig. S3†). Meanwhile, the concentration of fluorophore **1** (retention time was 4.19 min) increased gradually.

To further examine whether the probe **AZO-Cy** was suitable for hypoxia detection, cytochrome P450 reductase catalyzed reduction was applied in an *in vitro* assay under different p_{O_2} (Fig. 3). In order to create a hypoxic environment, a mixed composition which contains argon and different concentrations of oxygen was bubbled into the **AZO-Cy** solution (1.0 μM, PBS buffer with 1% DMSO, pH 7.4) for 45 min, then cytochrome P450 reductase was added. Upon the addition of NADH (100 μM, as a cofactor of cytochrome P450 reductase) and CPR, a dramatic fluorescence enhancement was observed at around 610 nm. Under different hypoxia conditions, the fluorescence was produced with different intensities. We can find that when the oxygen concentration decreases, there is a significant nonlinear increase in fluorescence intensity. The experiment also demonstrated probe **AZO-Cy** could be used for detection of hypoxic cells.

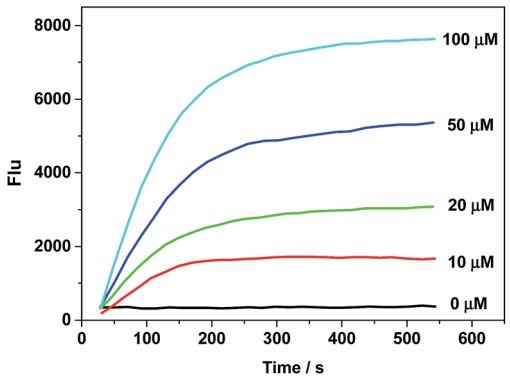

Fig. 2 Fluorescence intensity changes ($F_{610\ nm}$) with λ_{ex} = 450 nm at 37 °C over an incubation time of 10 min at varied concentrations of **AZO-Cy**: 0 (control), 10, 20, 50 and 100 μM. The measurements were performed in PBS buffer with 1.0 U mL^{-1} CPR and 100 μM of NADH.

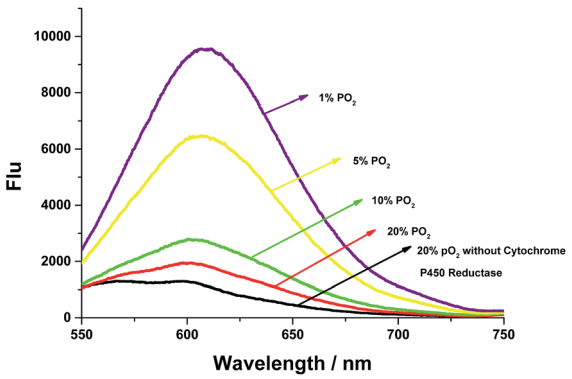

Fig. 3 Fluorescence changes of **AZO-Cy** without (purple curve) or with (other curves) various oxygen levels. The spectra were measured in phosphate buffer (pH 7.4 with 1% DMSO, containing 0.1 mM NADH) at 37 °C.

3.4 Selective response of probe AZO-Cy

To further evaluate the application in living cells, the anti-interference experiment also should be considered. Probe **AZO-Cy** was treated with reductants (VC and glutathione), biothiols (cysteine and dithiothreitol), inorganic salts ($FeCl_2$), glucose, NADH or amino acid (tyrosine). As shown in Fig. S2,† a noticeable fluorescence signal was observed even when the concentration of interference substances is up to 50 equiv. Therefore, it can be concluded that **AZO-Cy** displayed high selectivity for bio-reductase and is stable in biological systems.

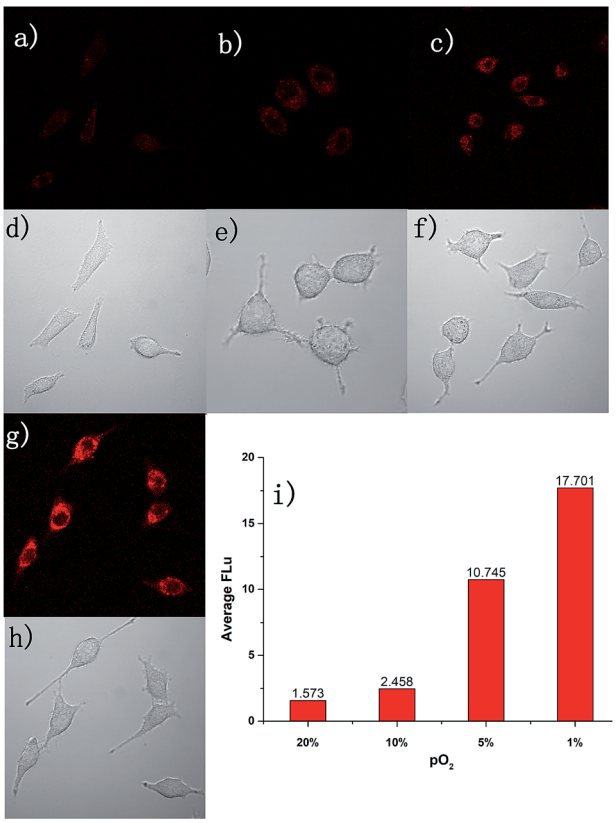

Fig. 4 Fluorescence microphotographs of A549 cells incubated with 1.0 μM fluorescent probe **AZO-Cy** at 37 °C. All the cells were incubated at different oxygen partial pressures; (a) and (d) were taken at aerobic condition (20% p_{O_2}). The others were taken at different hypoxic conditions: (b) and (e) were at 10% p_{O_2}; (c) and (f) were at 5% p_{O_2}; (g) and (h) were at 1% p_{O_2}, respectively. (d) (e) (f) and (h) were taken with bright field illumination; (a) (b) (c) and (g) were taken in fluorescence mode (red). (i) The mean fluorescence photons and relative ratio. Image J software gave an average emission value of fluorescence photons.

Open Access Article. Published on 11 ervence 2019. Downloaded on 17.12.2025 17:34:02.
This article is licensed under a Creative Commons Attribution-NonCommercial 3.0 Unported Licence.

3.5 Hypoxic cell imaging

Due to the excellent performance in different p_{O_2} experiments and anti-interference capability, we carried out a cell imaging experiment to detect different hypoxic conditions in cancer cells. As shown in Fig. 4, under normoxia conditions (p_{O_2} is 20%), the fluorescence intensity was weak. With the strengthening of the degree of hypoxia (from 10% to 1%), the fluorescence intensity was increased gradually. This experiment showed **AZO-Cy** was sensitive enough to the p_{O_2}. With Image J™ software (1.47v), the average fluorescence intensity value at different oxygen conditions was calculated (Fig. 4i). The mean fluorescence intensity increased from 1.573 to 17.701, nearly about an 11-fold increase.

For further evaluation of probe **AZO-Cy** applied in hypoxia imaging in cancer cells, A549 cell lines were also chosen for cellular fluorescence imaging in the presence of inhibitor diphenyliodonium chloride (DPIC). As shown in Fig. 5, under hypoxic conditions (1% p_{O_2}), even in the presence of low concentrations of inhibitor, a weak fluorescence signal was also observed. The fluorescence intensity is about 64% percent in the presence of the inhibitor compared to the routine experiment under hypoxic conditions. This experiment further proved that even in the presence of an inhibitor of CPR, part of the probe **AZO-Cy** was also reduced under hypoxic conditions.

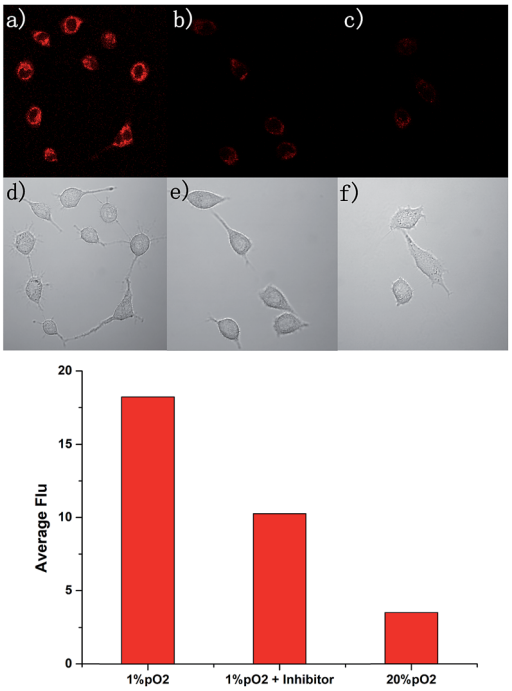

Fig. 5 Fluorescence microphotographs of A549 cells incubated with 1.0 μM fluorescent probe **AZO-Cy** at 37 °C. All of the cells were incubated under different conditions: (a) and (d) were taken under hypoxic conditions (1% p_{O_2}); (b) and (e) were taken under hypoxic conditions (1% p_{O_2}) and the cells were incubated with inhibitor; (c) and (f) were taken under aerobic conditions (20% p_{O_2}). The first row was taken in fluorescence mode (red) (a–c); and the second row was taken with bright field illumination.

4 Conclusion

In summary, we present a new design concept for a hypoxia fluorescence probe in which the functional group was conjugated to the indole group (electron-deficient side). In enzyme experiments, **AZO-Cy** had a good ability to distinguish oxygen concentration rapidly and sensitively in the presence of NADH. The fluorescence intensity in hypoxic conditions is about 11-fold stronger than aerobic conditions. Enzyme activity inhibition experiments indicated that CPR is not the only reductase that can reduce the azo bond. The azo bond as a functional group for hypoxia detection needs further study.

Conflicts of interest

There are no conflicts to declare.

Acknowledgements

We thank the National Natural Science Foundation of China (31570360 and 31702070) for financial support. This work was also sponsored by Program of Shanghai Academic/Technology Research Leader (17XD1423000) and by Shanghai Rising-Star Program (18QB1404000).

Notes and references

1 R. Choudhury, *Int. J. Gen. Med.*, 2018, **11**, 431–442.
2 A. Schurich, I. Magalhaes and J. Mattsson, *Immunotherapy*, 2019, **11**, 335–345.
3 V. Petrova, M. Annicchiarico-Petruzzelli, G. Melino and I. Amelio, *Oncogenesis*, 2018, **7**, 10.
4 H. Kim, Q. Lin, P. M. Glazer and Z. Yun, *Breast Cancer Res.*, 2018, **20**, 16.
5 M. C. Simon, *Cancer Res.*, 2016, **76**, IA13.
6 C. Ward, S. P. Langdon, P. Mullen, A. L. Harris, D. J. Harrison, C. T. Supuran and I. H. Kunkler, *Cancer Treat. Rev.*, 2013, **39**, 171–179.
7 K. Teramoto, Y. Kataoka, T. Igarashi, Y. Ohshio, J. Hanaoka and Y. Daigo, *Cancer Res.*, 2015, **75**, 5080.
8 P. R. de Jong, A. D. Campos, S. L. Shanahan, A. Richardson and G. Powis, *Cancer Res.*, 2016, **76**, A25–A25.
9 Q. Cai, T. Yu, W. P. Zhu, Y. F. Xu and X. H. Qian, *Chem. Commun.*, 2015, **51**, 14739–14741.
10 K. Kiyose, K. Hanaoka, D. Oushiki, T. Nakamura, M. Kajimura, M. Suematsu, H. Nishimatsu, T. Yamane, T. Terai, Y. Hirata and T. Nagano, *J. Am. Chem. Soc.*, 2010, **132**, 15846–15848.
11 K. Y. Zhang, P. L. Gao, G. L. Sun, T. W. Zhan, X. L. Li, S. J. Liu, Q. Zhao, K. K. W. Lo and W. Huang, *J. Am. Chem. Soc.*, 2018, **140**, 7827–7834.
12 S. Z. Luo, R. F. Zou, J. C. Wu and M. P. Landry, *ACS Sens.*, 2017, **2**, 1139–1145.
13 R. Stoyanova, K. Huang, K. Sandler, H. Cho, S. Carlin, P. B. Zanzonico, J. A. Koutcher and E. Ackerstaff, *Transl Oncol.*, 2012, **5**, 437–U114.

This journal is © The Royal Society of Chemistry 2019

Open Access Article. Published on 11 ervence 2019. Downloaded on 17.12.2025 17:34:02.
This article is licensed under a Creative Commons Attribution-NonCommercial 3.0 Unported Licence.

14 T. A. M. Egeland, K. Gulliksrud, J. V. Gaustad, B. Mathiesen and E. K. Rofstad, *Magn. Reson. Med.*, 2012, **67**, 519–530.
15 C. T. Lee, M. K. Boss and M. W. Dewhirst, *Antioxid. Redox Signaling*, 2014, **21**, 313–337.
16 D. Yang, H. Y. Tian, T. N. Zang, M. Li, Y. Zhou and J. F. Zhang, *Sci. Rep.*, 2017, **7**, 9174.
17 Y. Fang, W. Shi, Y. M. Hu, X. H. Li and H. M. Ma, *Chem. Commun.*, 2018, **54**, 5454–5457.
18 A. Chevalier, P. Y. Renard and A. Romieu, *Chem.–Asian J.*, 2017, **12**, 2008–2028.
19 L. Cui, Y. P. Shi, S. P. Zhang, L. L. Yan, H. Zhang, Z. R. Tian, Y. Y. Gu, T. Guo and J. H. Huang, *Dyes Pigm.*, 2017, **139**, 587–592.
20 S.-Y. Na, S. Park, S.-Y. Kim and H.-J. Kim, *Dyes Pigm.*, 2019, **161**, 247–251.
21 W. Piao, S. Tsuda, Y. Tanaka, S. Maeda, F. Y. Liu, S. Takahashi, Y. Kushida, T. Komatsu, T. Ueno, T. Terai, T. Nakazawa, M. Uchiyama, K. Morokuma, T. Nagano and K. Hanaoka, *Angew. Chem. Int. Ed.*, 2013, **52**, 13028–13032.
22 X. Li, J. Cheng, Y. L. Gong, B. Yang and Y. Z. Hu, *Biosens. Bioelectron.*, 2015, **65**, 302–306.
23 Y. Zhou, M. Maiti, A. Sharma, M. Won, L. Yu, L. X. Miao, J. Shin, A. Podder, K. N. Bobba, J. Han, S. Bhuniya and J. S. Kim, *J. Controlled Release*, 2018, **288**, 14–22.
24 T. Guo, L. Cui, J. N. Shen, W. P. Zhu, Y. F. Xu and X. H. Qian, *Chem. Commun.*, 2013, **49**, 10820–10822.
25 N. Kwon, M. K. Cho, S. J. Park, D. Kim, S. J. Nam, L. Cui, H. M. Kim and J. Yoon, *Chem. Commun.*, 2017, **53**, 525–528.
26 J. Zhang, H. W. Liu, X. X. Hu, J. Li, L. H. Liang, X. B. Zhang and W. Tan, *Anal. Chem.*, 2015, **87**, 11832–11839.
27 S. H. Luo, Y. C. Liu, F. Y. Wang, Q. Fei, B. Shi, J. C. An, C. C. Zhao and C. H. Tung, *Analyst*, 2016, **141**, 2879–2882.
28 P. Verwilst, J. Han, J. Lee, S. Mun, H. G. Kang and J. S. Kim, *Biomaterials*, 2017, **115**, 104–114.